



HAL
open science

Optical model-based calibration of gray levels for laser damage size assessment

Guillaume Hallo, Chloé Lacombe, Marin Fouchier, Myriam Zerrad, Jérôme Néauport, François Hild

► **To cite this version:**

Guillaume Hallo, Chloé Lacombe, Marin Fouchier, Myriam Zerrad, Jérôme Néauport, et al.. Optical model-based calibration of gray levels for laser damage size assessment. *Optics Letters*, 2023, 48 (2), pp.481-484. 10.1364/OL.481048 . hal-03911646

HAL Id: hal-03911646

<https://hal.science/hal-03911646v1>

Submitted on 23 Dec 2022

HAL is a multi-disciplinary open access archive for the deposit and dissemination of scientific research documents, whether they are published or not. The documents may come from teaching and research institutions in France or abroad, or from public or private research centers.

L'archive ouverte pluridisciplinaire **HAL**, est destinée au dépôt et à la diffusion de documents scientifiques de niveau recherche, publiés ou non, émanant des établissements d'enseignement et de recherche français ou étrangers, des laboratoires publics ou privés.

Optical model-based calibration of gray levels for laser damage size assessment

GUILLAUME HALLO^{1,2,*}, CHLOÉ LACOMBE¹, MARIN FOUCHIER³, MYRIAM ZERRAD³, JÉRÔME NÉAUPORT¹, AND FRANÇOIS HILD²

¹CEA, CESTA, F-33116 Le Barp, France

²Université Paris-Saclay, CentraleSupélec, ENS Paris-Saclay, CNRS, LMPS - Laboratoire de Mécanique Paris-Saclay, Gif-sur-Yvette, France

³Aix Marseille Univ, CNRS, Centrale Marseille, Institut Fresnel, Marseille, France

*Corresponding author: guillaume.hallo@cea.fr

Compiled December 21, 2022

Fused silica is prone to damage under ultraviolet laser irradiation. Because they are key components to achieve fusion on high energy laser facilities, final fused silica optics are analyzed after each laser shot. The quantification of damage sites is limited by the image resolution. Measurements of scattered light by damage sites allow for sub-pixel detection and growth monitoring after a calibration step based on time-consuming measurements laser facilities. It is proven herein that modeling laser damage size monitoring based on light scattering is efficient to link gray levels to damage diameters, thereby avoiding any experimental calibration based on a reference optics on the facility. © 2022 Optica Publishing Group

<http://dx.doi.org/10.1364/ao.XX.XXXXXX>

High power laser facilities such as the National Ignition Facility (NIF), ShenGuang-III (SG-III) and Laser MegaJoule (LMJ) were designed to achieve fusion by inertial confinement [1–3]. For each laser beam, multi-kilojoule ultraviolet (UV) laser energy with nanosecond pulse duration is required. Under such extreme laser conditions, optical components made of fused silica are prone to laser-induced damage [4]. Once a damage site has initiated, it grows after each UV laser shot since the laser energy is greater than the growth threshold, which is usually the case for fusion scale laser facilities [5]. To some extent, the performances of such large installations are therefore limited by laser-induced damage of final optics [6]. To partially overcome this issue, two complementary methods were developed, namely, Carbon Dioxide (CO₂) laser optics mitigation and local laser shadowing [7]. CO₂ laser optics mitigation is possible as long as the damage size is less than 750 μm. However, the mitigation requires the optics to be removed from the facility. Small parts of the laser beam may be shaded to stop the growth of critical damage sites, and therefore dictate the number of optics removals. Hence, it is necessary to detect damage sites and quantify their growth before they reach the mitigation limit. In order to be sure that no damage site reaches the mitigation limit (750 μm in diameter), a corresponding safety margin of about a factor 2 on the estimated

damage diameter is taken, so that the limit used at LMJ is 300 μm. This margin takes into account the measurement error on the diameter as well as the possibility for a damage site to exceed 750 μm in diameter after one supplementary laser shot with high fluence. Images of the final optics are acquired after each laser shot using similar imaging systems at NIF, SG-III and LMJ [7–9]. The optics are illuminated from the edge. Light is internally trapped in the optics until it reaches a damage site that scatters it. A part of the scattered light from damage sites is collected by the imaging system at a distance of 8 m. The acquired images are dark-fields with bright spots corresponding to damage sites. The image resolution ($\approx 100 \mu\text{m}/\text{pixel}$) is not sufficient to accurately measure the diameter of damage sites less than 300 μm by counting the number of lit pixels in the image. This low accuracy on diameter measurements is not compatible with damage growth quantification required for efficient mitigation.

Light scattering methods are widely used to estimate the size of proteins [10]. To measure damage growth with sub-pixel resolution without modifying the imaging and acquisition systems, one proposed solution is to use the gray levels of acquired images due to damage light scattering [7]. However, images may suffer from some disturbances [11]. Techniques based on Digital Image Correlation (DIC) principles were proposed to correct these acquired images. After corrections, the pixel intensity variations are only affected by damage growth and acquisition noise [11]. Since light scattering from molecules allows their radius of gyration and weight to be estimated, the signals emitted by light scattering from laser damage sites may provide information about their diameter, depth and possibly their growth. Thanks to an image calibration process, it was shown that integrated gray levels were positively correlated to damage sizes [7]. This calibration process required an optical component to be prepared with numerous laser damage sites with different sizes, to be mounted on the installation, and images of the damaged optic to be acquired. In the busy operational schedule of large fusion-scale laser facilities, this method is time-consuming, especially since this calibration must be performed for each of the laser beams due to possible variations in lighting conditions.

In this paper, an optical model-based calibration is proposed to estimate damage diameters from gray levels instead of using a reference optics mounted on the facility. The optical model

of the image acquisition process makes gray level simulations possible. The model may be used after revision or potential structural modification of the acquisition system to avoid a new online time-consuming calibration. It is based on damage light scattering measurements, optical simulation of the lighting system, and a numerical model of the image acquisition system. The image acquisition system of laser-induced damage on LMJ final optics is first described. Each step of the modeling process is presented, namely, lighting system, light scattering by damage sites, and imaging system. An image of a vacuum window with 930 damage sites was acquired on the LMJ facility to be used as reference for the simulations. The results are presented and compared to the reference image to assess experimental-free, model-based only, damage size measurements from gray levels.

The monitored 176 final optics at LMJ, among which the so-called vacuum windows, are distributed all around the 8 m in radius experiment chamber. A vacuum window is a 40 cm large optical component. To make damage sites visible, each vacuum window is illuminated by 2 green Light-Emitting Diodes (LEDs) mounted on one edge of the components. Such LEDs have a maximum emissivity at 525 nm wavelength. Light provided by the LEDs enters into the optics and illuminates the rear and front sides of the vacuum windows. Aluminum alloy frames maintain the optical components. The light that reaches the frame is reflected in the vacuum window. Laser damage sites, mainly located on the front face, scatter light. A part of this scattered light is collected by an objective lens that images vacuum windows on a Charge Coupled Device (CCD) sensor. It converts the collected light energy into gray levels. The image acquisition configuration is shown in Figure 1(a). The optical model presented hereafter is divided into several parts (lighting system, light scattering by damage sites and imaging system). Using the proposed model, the integrated pixel intensity of a damage site is expressed as a function of damage site size and lighting parameters. The two LEDs, the fused silica vacuum window and its aluminum alloy frame were considered as the lighting system. The following simplifying assumptions were made, namely, reflections on the frame were considered as specular, screws and other small mounting devices of the frame were removed from the model for ray tracing considerations, optical anti-reflection coating in the UV wavelength of the vacuum window was not modeled. Under these assumptions, the input data of the lighting system model were the parameters of Nichia NSPG500DS LED (wavelength emissivity, angular distribution of emission, light intensity), the geometry of a vacuum window with beveled corners made of fused silica (Heraeus Suprasil), the simplified geometry and reflectivity of the optical frame in aluminum alloy. These input data were implemented in the ray tracing software Zemax OpticStudio in a non-sequential mode [12]. A square matrix of 100 rectangular detectors collected the incident radiance [$\text{Wm}^{-2}\text{sr}^{-1}$] on the front face of the vacuum window for several positions on the surface as shown as orange boxes in Figure 1(b).

Once the previously simulated incident light reached a damage site, the latter scattered it according to the Bidirectional Scattering Distribution Function (BSDF) [13, 14]. The BSDF links the scattered radiance by a surface, L_s [$\text{Wm}^{-2}\text{sr}^{-1}$], and the incident irradiance on the surface, E_i [Wm^{-2}], for the incident angles θ_i and ϕ_i , as well as the scattered angles θ_s and ϕ_s (spherical coordinate system)

$$BSDF(\theta_i, \phi_i, \theta_s, \phi_s) = \frac{dL_s(\theta_i, \phi_i, \theta_s, \phi_s)}{dE_i(\theta_i, \phi_i, \theta_s, \phi_s)} \quad (1)$$

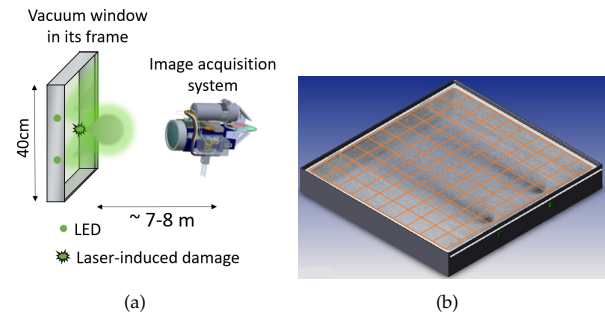


Fig. 1. (a) Schematic view of image acquisition for an LMJ vacuum window. (b) Result of OpticStudio (Zemax) simulation with the described lighting system model. The matrix of detectors is shown as orange squares. The distribution of simulated incident light energy on the face of the window is displayed.

To simulate the amount of scattered light toward the imaging system, the BSDF, a quantity corresponding to the illuminated object and independent of the lighting system, needs to be known. It was proposed to measure the dispersion as a function of angle, and to relate it to surface statistics [15]. Since then, many works linked the surface roughness to the scattering function from smooth to rough surfaces [14]. However, the validity of these models was limited to surface scattering. A damage site can be seen as a crater in hundreds of micrometers with sub-surface cracks [16]. Scattering surface models did not take into account the interaction between crater scattering (surface) and sub-surface crack scattering (volume).

It is also possible to measure directly the BSDF of a sample in reflection and transmission [14]. In this paper, it was chosen to measure the BSDF of 12 damage sites whose diameters ranged from 100 μm to 700 μm . The 12 damage sites were initiated with a 1064 nm wavelength laser at 8 ns pulse duration on circular fused silica wafers (1 mm in thickness and 10 cm in diameter) with no optical coating. Two sites, 5 cm apart and 2.5 cm from the wafer edge, were created. For larger sites, multi-laser shots were performed to grow the sites to the specified size. Despite the damage mechanisms being different between ultraviolet and infrared wavelengths, damage sites initiated at wavelengths of 351 nm and 1064 nm were both described as molten craters beneath which occurred fractures similar to Hertzian cone cracks for diameters greater than 200 μm [17, 18]. This is the reason why the simulation was based on the BSDFs measured for the 5 largest damage sites, *i.e.*, diameters greater than 200 μm . Two of them are shown in Figure 2. The scattering measurements were

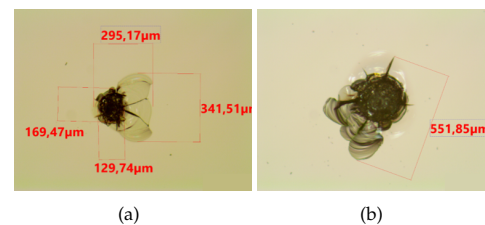


Fig. 2. Images of 2 laser damage sites whose BSDF was measured. The different shapes of the sites are considered as representative of those observed on LMJ vacuum windows.

performed with the Spectral and Angular Light Scattering characterization Apparatus in its 4th configuration (SALSA 4) [19]. The measured quantity with SALSA 4 is the Angle Resolved Scattering (ARS)

$$ARS(\theta_i, \phi_i, \theta_s, \phi_s) = BSDF(\theta_i, \phi_i, \theta_s, \phi_s) \cos(\theta_i) \quad (2)$$

The BSDFs were measured for all damage sites at 525 nm wavelength, which matched the maximum emissivity of the LMJ lighting system. The lighting conditions of the damage sites were different in laser facilities (from the edge) and SALSA 4 (a 6 mm in diameter laser beam illuminated the damage site whose ARS was measured at several angles). The beam was sufficiently large to fully illuminate each damage site during the measurements. The BSDF of undamaged fused silica was measured to be 1000 times lower than that of damage sites. Thus, the scattered light by undamaged silica was not taken into account in the simulations. The energy of light collected by the objective lens of the LMJ imaging system was computed using ARS measurements and the simulated incident radiance. The scattered radiance of a damage site toward the objective of the imaging system reads

$$L_s = 4\pi^2 \int_{\theta_i} \int_{\phi_i} \int_{\theta_s} ARS(\theta_i, \phi_i, \theta_s) L_i(\theta_i, \phi_i) d\theta_i d\phi_i d\theta_s \quad (3)$$

for $\theta_i \in [0; \frac{\pi}{2}]$; $\theta_s \in [\pi - \alpha, \pi]$ and $\phi_s \in [0, 2\pi]$, where α is the object aperture angle of the objective lens. The scattered flux toward the objective lens Φ_s [W] reads

$$\Phi_s = L_s \cos(\theta_{obj}) A_d 2\pi (1 - \cos(\alpha)) \quad (4)$$

where L_s [$\text{Wm}^{-2}\text{sr}^{-1}$] is the scattered radiance toward the objective, A_d [m^2] the area of the damage site, α the objective aperture angle, and θ_{obj} the angle between the normal axis to the face of the vacuum window and the optical axis of the camera. The scattered flux to the objective lens was considered as constant over the acquisition time of the camera Δ_t [s]. Thus, the scattered light energy, E_s [J] toward the objective lens reduced to

$$E_s = \Phi_s \Delta_t \quad (5)$$

Once the scattered energy toward the objective lens was computed, the integrated signal of gray levels was obtained by modeling the CCD sensor. Several conversions were performed (light energy to photons to electrons to gray levels). The total integrated signal (TIS) reads

$$\text{TIS} = w \frac{E_s QE}{h\nu F_c} \quad (6)$$

where the coefficient w is a constant weight used to calibrate the model on measurements, E_s the scattered light energy, QE the Quantum Efficiency of the CCD sensor, h Planck's constant, ν the frequency of light, and F_c the conversion factor from electrons to gray levels of the CCD sensor. The purpose of the coefficient w was to compensate for errors due to the lack of exact knowledge of some system parameters.

To validate the results of simulations using the above mentioned model, 930 damage sites were initiated on a new vacuum window. A Nd:YAG laser set-up was used to initiate damage sites [20]. Damage site diameters were measured with an optical microscope before the component was mounted on the facility. The diameters of these sites ranged between 50 μm and 270 μm , and they are referred to as true diameters. An image of this optical component illuminated by the lighting system was acquired by the imaging device once it was mounted on the LMJ

beam. The TIS was measured for each damage site by summing the gray levels of lit pixels describing the damage site in the acquired image. It is plotted as a function of the true diameter of damage sites in Figure 3.

The incident light is collected by the area of each damage site. The flux scattered by a damage site is proportional to its surface area (see Eq. (4)). Thus, it was chosen to interpolate the measured TIS with a square power law in diameter (*i.e.*, linear in area)

$$\text{TIS}_m = \kappa \left(\frac{D}{D_0} \right)^2 \quad (7)$$

where D denotes the diameter of the damage site, D_0 the physical size of one pixel (100 μm), and κ the scale parameter equal to 3.5×10^3 gray level. The estimated diameter using TIS was directly obtained from Eq. (7).

The TIS of 5 damage sites (including a, b in Figure 2) were simulated for the 100 positions on the vacuum window corresponding to the 100 rectangular detectors used to collect the incident radiance in the simulation. The damage diameters for the simulation varied from 230 μm to 550 μm , corresponding to about the largest size where damage mitigation was possible (white area in Figure 3). The simulated TIS_s was also interpolated by the same power law. As shown in Figure 3, for any size of the damage sites, all TIS obtained by simulation or acquisition were in agreement with Eq. (7). The proposed model was deemed efficient to simulate TIS measured by the LMJ acquisition system. For most damage sites, the greater the incident light energy, the higher the TIS. However, some exceptions were observed, which were presumably due to model approximations, morphology differences or scattering interactions between sites.

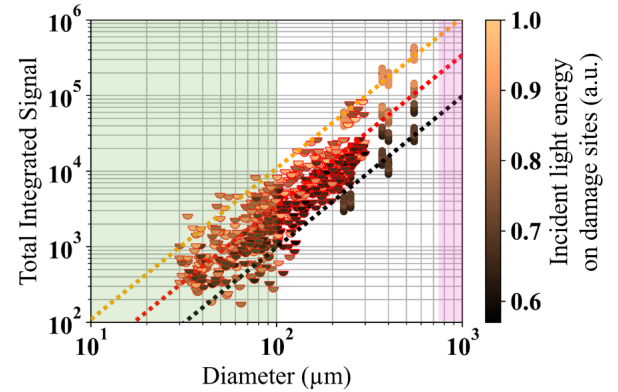
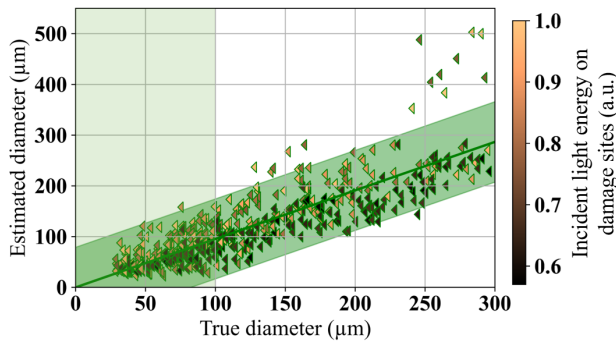


Fig. 3. Measured TIS_m on the acquired image for each damage site as a function of its diameter (half circles with red edge). The color bar indicates the incident light energy on each damage site in arbitrary units. The measured results are interpolated by Eq. (7) (red dotted line). Simulated TIS_s for 5 damage sites as a function of their diameters (full circle markers). The orange (resp. dark) dashed line indicates the best fit of TIS_s for the 10% brightest (resp. least illuminated) areas on the vacuum window with $\kappa = 10^4$ (resp. $\kappa = 10^3$). The green (resp. pink) area indicates damage mitigation less than the image resolution (resp. for which damage mitigation is no longer possible).

Figure 4 shows the result of diameter estimation using the TIS values for damage diameters ranging between 30 μm and

300 μm . These diameters corresponded to sizes where a decision
 301 about damage mitigation had to be made. Measuring diameters
 302 by TIS led to correct estimations of the true size of damage.
 303 It is worth noting that the 95% prediction interval (P.I.) was
 304 $\pm 68 \mu\text{m}$. The 95% P.I. is an estimate of an interval in which
 305 a future diameter estimation will fall with a 95% probability.
 306 Diameter estimations by TIS were accurate up to damage sizes of
 307 $200 \mu\text{m}$, which indicates that it is a convenient way of monitoring
 308 damage initiation and early growth.



309 **Fig. 4.** Estimated diameters of each damage sites from TIS (left
 310 triangle with green edge). The green line indicates a linear
 311 interpolation of estimated diameters. The green area shows
 312 the 95% P.I. of the estimated diameters.

313 A large scatter of TIS over one decade was observed for identical
 314 damage sizes in the current LMJ configuration of lighting and
 315 acquisition systems, either by measurement or by simulation.
 316 This scatter is related to the light energy received by the
 317 damage sites depending on their position on the vacuum window
 318 (Figure 3), mainly due to nonuniform light distribution on the
 319 damaged face of the vacuum window induced by the twin LED
 320 system (Figure 1). These results indicate that the current
 321 lighting system itself was not sufficient to provide an invariant
 322 TIS measurement according to the damage site position on the
 323 vacuum window. However, diameter was measured accurately
 324 by coupling measured TIS for a damage site and its position
 325 on the optical component using the proposed model and simulations.
 326 Despite taking into account the TIS and the position of the
 327 damage sites, differences in light scattering between 2
 328 sites of the same size induced an uncertainty on the size
 329 measurement ($\pm 68 \mu\text{m}$ for true diameters varying between $30 \mu\text{m}$
 330 and $300 \mu\text{m}$). The value $\pm 68 \mu\text{m}$ was due to the technique of
 331 measuring diameters from TIS and the quality of the lighting system,
 332 not the calibration method. It was thus demonstrated that
 333 model-based calibrations achieved the same accuracy as in-situ
 334 measurement-based calibration but at a lower operational costs
 335 for laser facilities. The scatter of diameter estimation for identical
 336 true diameters may also be due to differences in damage
 337 morphology involving differences in light scattering.

338 Beyond the current system modeling, the proposed approach
 339 allows modifications of lighting or image acquisition systems
 340 to be virtually tested and evaluated, be it at LMJ, NIF, or SG-III
 341 facilities, or any other installation interested in accurately
 342 monitoring damage growth by acquiring light scattering signals.

343 A model was proposed to simulate the TIS to quantify the
 344 size of laser-induced damage sites on fused silica optics of high
 345 energy laser facilities. The model was based on three steps,

346 namely, (i) lighting system modeling using a ray tracing software,
 347 (ii) measurements of light scattering by damage sites, and
 348 (iii) numerical imaging system modeling. The TIS simulations
 349 using the proposed model were calibrated and validated on
 350 an acquired image that contained 930 damage sites whose size
 351 was precisely measured using an optical microscope before the
 352 component was mounted on the facility. The measured TIS on
 353 the acquired image proved that the LMJ lighting system itself
 354 was not sufficient to measure accurately damage sizes with TIS
 355 alone. It was evidenced that model-based calibration achieved
 356 the same accuracy as in-situ measurement-based calibration but
 357 at a significantly lower operational costs for laser facilities.

358 The proposed model is currently used to virtually test system
 359 modifications in order to improve damage size measurements.
 360 Although the paper focused on the damage monitoring system of
 361 LMJ, the proposed approach may be utilized to model and
 362 simulate the performance of other systems based on the
 363 measurement of light scattering signals. Using such model, time-
 364 consuming online measurements were avoided to calibrate TIS
 365 levels with the size of scattering objects (such as damage sites).

366 **Acknowledgments.** The authors would like to thank Richard-
 367 Nicolas Verrone and Konstantinos Iliopoulos for the damage sites on
 368 the wafers, and all the people who prepared the vacuum window.

369 **Disclosures.** The authors declare no conflicts of interest.

370 **Data Availability Statement.** Data underlying the results presented
 371 in this paper are not publicly available at this time but may be obtained
 372 from the authors upon reasonable request.

373 REFERENCES

- 374 1. G. Miller, E. Moses, and C. Wuest, *Opt. Eng.* **43**, 2841 (2004).
- 375 2. X. He and W. Zhang, *EPJ Web Conf.* **59**, 01009 (2013).
- 376 3. J. Ebrardt and J. Chaput, *J. Physics: Conf. Ser.* **112**, 032005 (2008).
- 377 4. L. Lamaignère, G. Dupuy, A. Bourgeade *et al.*, *Appl. Phys. B: Lasers Opt.* **114**, 517 (2014).
- 378 5. K. Manes, K. R. Manes, M. L. Spaeth *et al.*, *Fusion Sci. Technol.* **69**, 146 (2016).
- 379 6. P. A. Baisden, L. J. Atherton, R. A. Hawley *et al.*, *Fusion Sci. Technol.* **69**, 295 (2016).
- 380 7. M. L. Spaeth, P. J. Wegner, T. I. Suratwala *et al.*, *Fusion Sci. Technol.* **69**, 265 (2016).
- 381 8. F. Wei, F. Chen, B. Liu *et al.*, *Opt. Eng.* **57**, 1 (2018).
- 382 9. G. Hallo, C. Lacombe, R. Parreault *et al.*, *Opt. Express* **29**, 35820 (2021).
- 383 10. K. Takeuchi, Y. Nakatani, and O. Hisatomi, *Open J. Biophys.* **4** (2013).
- 384 11. G. Hallo, C. Lacombe, J. Néauport *et al.*, *Opt. Lasers Eng.* **146**, 106674 (2021).
- 385 12. Zemax LLC, "Opticstudio," (2015).
- 386 13. F. E. Nicodemus, J. C. Richmond, J. J. Hsia *et al.*, *Geometrical Considerations and Nomenclature for Reflectance* (Jones and Bartlett Publishers, Inc., USA, 1992), p. 94–145.
- 387 14. J. Stover, *Optical Scattering: Measurement and Analysis*, Press Monographs (SPIE Press, 2012).
- 388 15. P. Beckmann and A. Spizzichino, "The scattering of electromagnetic waves from rough surfaces," (1963).
- 389 16. M. Veinhard, O. Bonville, R. Courchinoux *et al.*, *Opt. Lett.* **42**, 5078 (2017).
- 390 17. M. Norton, J. Adams, C. Carr *et al.*, *Proc. SPIE - The Int. Soc. for Opt. Eng.* **6720** (2008).
- 391 18. J. Han, Q. Zhang, R. Niu *et al.*, *Opt. Eng.* **51**, 121809 (2012).
- 392 19. M. Fouchier, M. Zerrad, M. Lequime *et al.*, *Opt. Lett.* **45**, 2506 (2020).
- 393 20. R. Diaz, R. Courchinoux, J. Luce *et al.*, *Appl. Phys. B - Laser Opt.* **121**, 439 (2015).

FULL REFERENCES

- 340
- 341 1. G. Miller, E. Moses, and C. Wuest, "The national ignition facility," *Opt.*
342 *Eng.* **43**, 2841–2853 (2004).
 - 343 2. X. He and W. Zhang, "Advances in the national inertial fusion program
344 of china," *EPJ Web Conf.* **59**, 01009– (2013).
 - 345 3. J. Ebrardt and J. Chaput, "Lmj project status," *J. Physics: Conf. Ser.*
346 **112**, 032005 (2008).
 - 347 4. L. Lamaignère, G. Dupuy, A. Bourgeade *et al.*, "Damage growth in
348 fused silica optics at 351 nm: refined modeling of large-beam experi-
349 ments," *Appl. Phys. B: Lasers Opt.* **114**, 517–526 (2014).
 - 350 5. K. Manes, K. R. Manes, M. L. Spaeth *et al.*, "Damage Mechanisms
351 Avoided or Managed for NIF Large Optics," *Fusion Sci. Technol.* **69**,
352 146–249 (2016).
 - 353 6. P. A. Baisden, L. J. Atherton, R. A. Hawley *et al.*, "Large optics for the
354 national ignition facility," *Fusion Sci. Technol.* **69**, 295–351 (2016).
 - 355 7. M. L. Spaeth, P. J. Wegner, T. I. Suratwala *et al.*, "Optics recycle loop
356 strategy for nif operations above uv laser-induced damage threshold,"
357 *Fusion Sci. Technol.* **69**, 265–294 (2016).
 - 358 8. F. Wei, F. Chen, B. Liu *et al.*, "Automatic classification of true and false
359 laser-induced damage in large aperture optics," *Opt. Eng.* **57**, 1 – 11
360 (2018).
 - 361 9. G. Hallo, C. Lacombe, R. Parreault *et al.*, "Sub-pixel detection of laser-
362 induced damage and its growth on fused silica optics using registration
363 residuals," *Opt. Express* **29**, 35820–35836 (2021).
 - 364 10. K. Takeuchi, Y. Nakatani, and O. Hisatomi, "Accuracy of protein size
365 estimates based on light scattering measurements," *Open J. Biophys.*
366 **4** (2013).
 - 367 11. G. Hallo, C. Lacombe, J. Néauport *et al.*, "Detection and Tracking of
368 Laser Damage Sites on Fused Silica Components by Digital Image
369 Correlation," *Opt. Lasers Eng.* **146**, 106674 (2021).
 - 370 12. Zemax LLC, "Opticstudio," (2015).
 - 371 13. F. E. Nicodemus, J. C. Richmond, J. J. Hsia *et al.*, *Geometrical Con-*
372 *siderations and Nomenclature for Reflectance* (Jones and Bartlett
373 Publishers, Inc., USA, 1992), p. 94–145.
 - 374 14. J. Stover, *Optical Scattering: Measurement and Analysis*, Press Mono-
375 graphs (SPIE Press, 2012).
 - 376 15. P. Beckmann and A. Spizzichino, "The scattering of electromagnetic
377 waves from rough surfaces," (1963).
 - 378 16. M. Veinhard, O. Bonville, R. Courchinoux *et al.*, "Quantification of
379 laser-induced damage growth using fractal analysis," *Opt. Lett.* **42**,
380 5078–5081 (2017).
 - 381 17. M. Norton, J. Adams, C. Carr *et al.*, "Growth of laser damage in fused
382 silica: Diameter to depth ratio," *Proc. SPIE - The Int. Soc. for Opt. Eng.*
383 **6720** (2008).
 - 384 18. J. Han, Q. Zhang, R. Niu *et al.*, "Effects of laser plasma on damage in
385 optical glass induced by pulsed lasers," *Opt. Eng.* **51**, 121809 (2012).
 - 386 19. M. Fouchier, M. Zerrad, M. Lequime *et al.*, "Wide-range wavelength
387 and angle resolved light scattering measurement setup," *Opt. Lett.* **45**,
388 2506–2509 (2020).
 - 389 20. R. Diaz, R. Courchinoux, J. Luce *et al.*, "Experimental evidence of
390 temporal and spatial incoherencies of Q-switched Nd:YAG nanosecond
391 laser pulses," *Appl. Phys. B - Laser Opt.* **121**, 439–451 (2015).